J|A|C|S
ARTICLES
Published on Web 10/05/2007

Conformational Manifold of α-Aminoisobutyric Acid (Aib) Containing Alanine-Based Tripeptides in Aqueous Solution Explored by Vibrational Spectroscopy, Electronic Circular Dichroism Spectroscopy, and Molecular Dynamics Simulations

Reinhard Schweitzer-Stenner,*,† Widalys Gonzales,† Gregory T. Bourne,‡ Jianwen A. Feng,‡ and Garland R. Marshall‡

Contribution from the Department of Chemistry, Drexel University, 3141 Chestnut Street, Philadelphia, Pennsylvania 19104 and Department of Biochemistry and Molecular Biophysics, Washington University, St. Louis, Missouri 63110

Received May 28, 2007; E-mail: RSchweitzer-Stenner@drexel.edu

Abstract: Replacement of the α-proton of an alanine residue to generate α-aminoisobutyric acid (Aib) in alanine-based oligopeptides favors the formation of a 3_{10} helix when the length of the oligopeptide is about four to six residues. This research was aimed at experimentally identifying the structural impact of an individual Aib residue in an alanine context of short peptides in water and Aib's influence on the conformation of nearest-neighbor residues. The amide I band profile of the IR, isotropic and anisotropic Raman, and vibrational circular dichroism (VCD) spectra of Ac-Ala-Ala-Aib-OMe, Ac-Ala-Aib-Ala-OMe, and Ac-Aib-Ala-Ala-OMe were measured and analyzed in terms of different structural models by utilizing an algorithm that exploits the excitonic coupling between amide I′ modes. The conformational search was guided by the respective ^{1}H NMR and electronic circular dichroism spectra of the respective peptides, which were also recorded. From these analyses, all peptides adopted multiple conformations. Aib predominantly sampled the right-handed and left-handed 3_{10}-helix region and to a minor extent the bridge region between the polyproline (PPII) and the helical regions of the Ramachandran plot. Generally, alanine showed the anticipated PPII propensity, but its conformational equilibrium was shifted towards helical conformations in Ac-Aib-Ala-Ala-OMe, indicating that Aib can induce helical conformations of neighboring residues positioned towards the C-terminal direction of the peptide. An energy landscape exploration by molecular dynamics simulations corroborated the results of the spectroscopic studies. They also revealed the dynamics and pathways of potential conformational transitions of the corresponding Aib residues.

Introduction

It is well-established that the natural, nonprotein amino acid α-aminoisobutyric acid (Aib, α-methylalanine) has a very high helix propensity and a high potential as a β-sheet (strand) breaker.[1−3] It is a common residue in peptides produced by microbes.[4,5] Examples are linear peptides of 15−20 residues, such as alamethicin, antiamoebin, and emerimicin, which produce voltage-gated channels in lipid membranes. Aib can be considered as being produced by the replacement of the C_α proton of an alanine residue by a methyl group which significantly limits the rotational degree of freedom with respect to the dihedral backbone coordinates ϕ and ψ. The Ramachandran plots reported by Marshall and Bosshard[6] and by Burgess and Leach[7] indicate two troughs of the potential energy landscape centered at ($\phi = -57°$, $\psi = -47°$) and ($\phi = 57°$, $\psi = 47°$), corresponding to right- and left-handed α-helices. Aib is *per se* achiral, but differential sampling of the two enantiomeric conformations corresponding to the above clusters in the Ramachandran plot are induced by neighboring chiral amino acid residues. The two clusters encompass both α-helices and 3_{10}-helices with a more frequent sampling of the latter for shorter peptides.

The 3_{10}-helix represents an important secondary structure in proteins and accounts for approximately 10% of helical residues in crystal structures (PDB).[8] Recent investigations of coil libraries indicate that 3_{10} rather than α is the preferred conformation in the lower left-handed Ramachandran quadrant of coil fragments of proteins.[9−11] The 3_{10}-helical segments in

† Drexel University.
‡ Washington University.

(1) Karle, I. L.; Balaram, P. *Biochemistry* **1990**, *29*, 6747.
(2) Moretto, V.; Crisma, M.; Bonora, G. M.; Toniolo, C.; Balaram, H.; Balaram, P. *Macromolecules* **1989**, *22*, 2939.
(3) Kumita, J. R.; Weston, C. J.; Choo-Smith, L.-P.; Wooley, G. A.; Smart, O. S. *Biochemistry* **2003**, *42*, 4492.
(4) Closse, A.; Huguenin, R. *Helv. Chim. Acta* **1974**, *57*, 533.
(5) Flippen, J. L.; Karle, I. L. *Biopolymers* **1976**, *15*, 1081.
(6) Marshall, G. R.; Bosshard, H. E. *Circ. Res.* **1972**, *30/31* (Suppl. II.), 143.
(7) Burgess, A. W.; Leach, S. J. *Biopolymers* **1973**, *12*, 2599.
(8) Barlow, D. J.; Thornston, J. M. *J. Mol. Biol.* **1988**, *201*, 601.
(9) Avbelj, F.; Baldwin, R. L. *Proc. Natl. Acad. Sci. U.S.A.* **2003**, *100*, 5742.
(10) Serrano, L. *J. Mol. Biol.* **1995**, *254*, 322−333.

proteins are generally short with an average length of four residues.[8,12] A 3_{10}-helix differs from the canonical α-helix not only with respect to its dihedral coordinates but also by a (*i*, *i* + 3) hydrogen-bonding arrangement.[13] Augspurger et al. investigated several Aib-based, aliphatic peptides of intermediate size in organic solvents and obtained a very thermostable 3_{10}-structure.[14] De Filippis et al. confirmed and explained the thermostability of Aib with the reduction of entropy of this amino acid residue in the unfolded state.[15] Numerous studies have been conducted to identify the conditions at which Aib stabilizes a 3_{10}-helix in peptides. Basically, a peptide gains an extra internal hydrogen bond in a 3_{10}-helix while steric interactions between residues favor α-helical torsional angles. At a critical length depending on the dielectric of the solvent, the two interactions approximately balance, and populations of both helices coexist. For this reason, short Aib-based peptides generally prefer 3_{10}-helices, whereas α-helices are more likely for longer peptides.[1,16,17] Rather long peptides, however, e.g., *p*BrBz-Aib_{10}-O*t*Bu (*p*BrBz, *para*-bromobenzyl; O*t*Bu, *tert*-butoxy) have been found to adopt 3_{10}-helices in crystals.[18] Balaram et al. used NMR and electronic circular dichroism spectroscopy to determine that the rather hydrophobic Boc-Aib-Val-Aib_2-Val_3-Aib-Val-Aib-OMe and Boc-Aib-Leu-Aib_2-Leu_3-Aib-Leu-Aib-OMe prefer the 3_{10} helix in $CDCl_3$, whereas an α-helix preference was found in $(CD_3)_2SO$.[19] This indicated that the solvent has a strong influence due to differences in dielectric constant and relative stabilities of hydrogen bonds on structural preference. Crystalline forces and the choice of the protection group have been identified as affecting the overall propensity of Aib-based peptides in crystals.[20−24] DiBlasio et al. found that crystallized (*p*BrBz-Aib-(Pro-Aib)$_n$-OMe ($n = 3, 4$) forms so-called *β*-ribbons which exhibit the Aib residues in 3_{10}-like conformations.[25] A review of the (mostly crystal) structure of a large number of Aib-containing peptides by Karle and Balaram indicated that the 3_{10}-helix is the preferred structure provided that the fraction of Aib residues exceeds 50%.[1] A dilution of the Aib content decreases the preference for 3_{10} so that a coexistence of both helix types is established. Smythe et al. calculated the potential energy landscape (i.e., potentials of mean force) and performed molecular dynamics calculations for (Ac-Aib_{10}-NHMe) *in vacuo*, water, and CH_3CN to obtain a higher stabilization of the α-helix for all three cases.[26] The stability of α_R was found to increase with the dielectric constant of the solvent. The higher stability of α_R was later confirmed by another computational study by Smythe et al.[27] However, MD simulations with the Cedar force field by Zhang and Hermans yielded nearly the opposite result in that these authors obtained 3_{10} as the predominant structure of Aib *in vacuo* and a $3_{10}/\alpha_R$ mixture in water.[28] A strong 3_{10} propensity of Aib was recently experimentally confirmed by Schievano et al.[29] Bürgi et al. used the GROMOS96 package to perform MD simulations for the octapeptide Z-Aib_5-Leu-Aib_2-OMe in DMSO and obtained a sampling of right- and left-handed helical conformations with comparable fractions of α-helical and 3_{10}-conformations.[30] A somewhat different result emerged from simulations of Mahadevan et al. for Aib_{10} in DMSO and water, for which the authors used the CHARMM22 force field.[31] They observed a mixture of α- and *π*-helix. Taken together, this review of the literature leads to the conclusion that more experimental data are required to obtain the α_R- and 3_{10}-propensity of Aib in peptides as well as the use of force fields that include multipole electrostatics and polarizability in MD simulations.[32]

In spite of some earlier work on short peptides, the intrinsic propensity of Aib as a guest in a natural host system has not yet been thoroughly investigated experimentally. Winter, Jung and colleagues reported the structure of crystallized Ac-Ala-Aib-Ala-OMe, Boc-Ala-Aib-Ala-OMe, and Boc-Gly-Ala-Aib-OMe.[33−35] For the two Ala-Aib-Ala peptides the authors identified a distorted *β*-turn. CD and NMR data indicate that this structure was maintained in DMSO for Boc-Ala-Aib-Ala-OMe. The crystal structure of Ac-Ala-Aib-Ala-OMe was of interest because the reported dihedral angles suggested that the central Aib adopts a 3_{10}-like conformation, whereas the two alanines exhibited a polyproline II (PPII)-like structure.[35] This is in accordance with the recently established PPII propensity of alanine in water.[36−38] The third peptide, Boc-Gly-Ala-Aib-OMe, was found to adopt a somewhat distorted 3_{10} or type III *β*-turn-like conformation.

Experiments reported in this paper were aimed at investigating the structure of three blocked Aib-containing tripeptides, namely Ac-Aib-Ala-Ala-OMe, Ac-Ala-Aib-Ala-OMe, and Ac-Ala-Ala-Aib-OMe in aqueous solution. Different vibrational spectroscopic techniques (IR, polarized Raman, vibrational circular dichroism (VCD)) were combined with ECD and ^{1}H NMR spectroscopy as well as molecular dynamics simulations.

(11) Duan, Y.; Wu, C.; Chowdhury, S.; Lee, M. C.;, Xiong, G.; Zhang, W.; Yang, R.; Cieplak, P.; Luo, R.; Lee, T.; Caldwell, J.; Wang, J.; Kollman, P. *J. Comput. Chem.* **2003**, *24*, 1999−2012.
(12) Robbins, D. J.; Stout, C. D. *Proteins: Struct., Funct., Genet.* **1989**, *5*, 289.
(13) Prasad, B. V. V.; Balaram, P. *CRC Crit. Rev. Biochem.* **1984**, *16*, 307.
(14) Augspurger, J. D.; Bindra, V. A.; Scheraga, H. A.; Kuki, A. *Biochemistry* **1995**, *34*, 2566.
(15) De Fillipis, V.; De Antoni, F.; Frigo, M.; de Laureto, P. P.; Fontana, A. *Biochemistry* **1998**, *37*, 1686.
(16) Bosch, R.; Jung, G.; Schmitt, H.; Winter, W. *Biopolymers* **1995**, *24*, 979.
(17) Tomicolo, C.; Bonora, G. M.; Bovaso, A.; Bendetti, E.; DiBlasio, B.; Pavone, V.; Pedone, C. *J. Biomol. Struct.* **1985**, *3*, 585.
(18) Pavone, V.; DiBasio, B.; Santini, A.; Benedetti, E.; Pedone, C. *J. Mol. Biol.* **1990**, *214*, 633.
(19) Balarram, H.; Sukumar, M.; Balaram, P. *Biopolymers* **1986**, *25*, 2209.
(20) Karle, I. L.; Flippen-Anderson, J. L.; Sakumer, M.; Balaram, P. *Int. J. Peptide Protein Res.* **1988**, *32*, 536.
(21) Karle, I. L.; Flippen-Anderson, J. L.; Sukumar, M.; Balaram, P. *J. Med. Chem.* **1992**, *35*, 3885.
(22) Marshall, G. R.; Hodgkin, E. E.; Langs, D. A.; Smith, G. D.; Zabrocki, J.; Leplawy, M. T. *Proc. Natl. Acad. Sci. U.S.A.* **1990**, *87*, 487.
(23) Blank, J. T.; Guerin, D.; Miller, S. J. *Org. Lett.* **2000**, *2*, 1248.
(24) Karle, I. L.; Sukumar, M.; Balaram, P. *Proc. Natl. Acad. Sci. U.S.A.* **1989**, *29*, 6747.
(25) DiBasio, B.; Pavone, V.; Savino, M.; Lombardi, A.; Nastri, F.; Pedone, C.; Benedetti, E.; Crisma, M.; Anzoli, M.; Toniolo, C. *J. Am. Chem. Soc.* **1992**, *114*, 6274.
(26) Smythe, M. L.; Huston, S. E.; Marshall, G. R. *J. Am. Chem. Soc.* **1993**, *115*, 11594.
(27) Smythe, M. L.; Huston, S. E.; Marshall, G. R. *J. Am. Chem. Soc.* **1995**, *117*, 5445.
(28) Zhang, L.; Herman, J. *J. Am. Chem. Soc.* **1994**, *116*, 11915.
(29) Schievano, E.; Bisello, A.; Chorev, M.; Bisol, A.; Mammi, S.; Peggion, E. *J. Am. Chem. Soc.* **2001**, *123*, 2743.
(30) Bürgi, R.; Daura, X.; Mark, A.; Bellanda, M.; Mammi, S.; Peggion, E.; van Gunsteren, W. *J. Peptide Res.* **2001**, *57*, 107.
(31) Mahadevan, J.; Lee, K.-H.; Kuczera, K. *J. Phys. Chem. B* **2001**, *105*, 1863.
(32) Ponder, J. W.; Case, D. A. Force fields for protein simulations. *Adv. Protein Chem.* **2003**, *66*, 27−85.
(33) Bosch, R.; Jung, G.; Winter, W. *Liebigs Ann. Chem.* **1982**, 1322.
(34) Jung, G.; Brückner, H.; Bosch, R.; Winter, W.; Schaal, H.; Strähle, J. *Liebigs Ann. Chem.* **1983**, 1096.
(35) Bosch, R.; Jung, G.; Voges, K.-P.; Winter, W. *Liebigs Ann. Chem* **1984**, 1117.
(36) Schweitzer-Stenner, R.; Eker, F.; Griebenow, K.; Cao, X.; Nafie, L. A. *J. Am. Chem. Soc.* **2004**, *126*, 2768.
(37) Schweitzer-Stenner, R.; Measey, T.; Kakalis, L.; Jordan, F.; Pizanelli, S.; Forte, C.; Greibenow, K. *Biochemistry* **2007**, *46*, 1587.
(38) Schweitzer-Stenner, R.; Measey, T. J. *Proc. Natl. Acad. Sci U.S.A.* **2007**, *104*, 6649−6654.

Analysis of the experimental results revealed the position-dependent propensity of Aib within an alanine context in water. Additionally, the influence of Aib on the conformational manifold sampled by its nearest neighbors was obtained. This is important for elucidating to what extent Aib affects the propensity of its nearest neighbors already in the unfolded state of peptides. The isolated-pair hypothesis often assumed in helix-coil transition theory stipulates that in the unfolded state the conformation of each amino acid residue is independent from that of its neighbors.[39] Pappu et al. have recently provided computational evidence that this hypothesis does not apply when a residue samples the right-handed helical region of the Ramachandran plot.[40] Since Aib doubtlessly prefers predominantly helical conformations, the set of peptides examined provided a convenient way to check these predictions experimentally.

Materials and Methods

Materials. Chlorotrityl resin (substitution = 1 mmol/g) and all N_α-Fmoc-amino acids (peptide-synthesis grade) were purchased from AdvanceChemtech (Louisville, KY) or Novabiochem (San Diego, U.S.A.). Diisopropylethylamine and trifluoroacetic acid were purchased from Aldrich (Milwaukee, USA). All other solvents including dichloromethane, *N*,*N*-dimethylformamide, and HPLC-grade acetonitrile were purchased from Fisher Scientific (USA).

Peptide Synthesis. All linear peptides were chemically synthesized stepwise using Fmoc protecting groups and *in situ* HBTU activation (or HATU for Aib) protocols as previously described.[41−43] Coupling efficiencies were determined by the quantitative ninhydrin test and recoupled where necessary to obtain >99.5% efficiency.[44]

Vibrational Spectroscopies. For IR, VCD, and Raman measurements, the peptides were dissolved at a concentration of 0.07 M (20.0 mg/mL) in D_2O with 0.025 M $NaClO_4$ and the ClO_4^- Raman peak at 934 cm^{-1} was used as an internal wavenumber standard.[45] All experiments were carried out at room temperature. The instrument for the Raman experiments has been described in detail in previous papers.[46] All spectra were recorded in the "continuous" mode and were measured a total of 8 times for each of the polarization directions. The spectra finally used for analysis were obtained by calculating the average of the measured spectra to improve the signal-to-noise ratio. The reference spectra of a 25 mM $NaClO_4$ in D_2O were subtracted from the respective sample spectra for both polarization directions.

The FTIR and VCD spectra were recorded with a Chiral IR Fourier Transform VCD spectrometer from BioTools. The instrument has been previously described.[46] The peptide sample was placed into a cell with a path length of 42 μm. The spectral resolution was 4 cm^{-1} for both spectra. The VCD and IR spectra were both collected as one measurement for a combined total time of 1440 min. To eliminate any background and solvent contributions to the IR spectrum, the cell was first filled with the reference solvent.

ECD Spectroscopy. The UV ECD spectra in the wavelength range of 180−240 nm of the peptides were measured as a function of temperature with an earlier described JASCO J-810 spectrapolarimeter[47] with 0.05 nm resolution and a scan speed of 500 nm/min. A 0.2 mm quartz cell was used for all experiments. We performed the measurements in D_2O rather than in H_2O (concentration 3 mM) in order to allow a direct comparison with structural data obtained by vibrational spectroscopies. The samples were placed in a nitrogen-purged JASCO CD module. The temperature at the cuvette was controlled by means of a Peltier type heating system with an accuracy of ±1 °C. For each measurement, the sample was allowed to equilibrate for 5 min at the adjusted temperature prior to acquisition. The spectra were obtained by averaging 10 scans and were collected as ellipticity as a function of wavelength and converted to difference molar absorptivities per residue as earlier described.[47]

Analysis of Vibrational Spectra: The spectral analysis program *MULTIFIT* was used to analyze all IR and Raman spectra.[48] Calibration of the Raman spectrum was checked using the $NaClO_4$ peak at 934 cm^{-1}. Reference spectra for both polarizations were measured which were subtracted from the relevant peptide spectra to eliminate solvent contributions. The isotropic and anisotropic Raman intensities were calculated as

$$I_{\mathrm{iso}} = I_x - \frac{4}{3} I_y$$
$$I_{\mathrm{aniso}} = I_y \qquad (1)$$

where I_x and I_y denotes the Raman scattering polarized light parallel and perpendicular to the polarization of the exciting laser.

Determination of $^3J_{C\alpha HNH}$ Coupling Constants. To determine the $^3J_{C\alpha HNH}$ coupling constants ^{1}H NMR spectra of Ac-Ala-Ala-Aib-OMe, Ac-Ala-Aib-Ala-OMe, and Ac-Aib-Ala-Ala-OMe were recorded at room temperature on a VARIAN 500 INOVA instrument in the Chemistry department of Drexel University. Pulse experiments used software supplied by VARIAN. The $^3J_{C\alpha HNH}$ coupling constant of the Aib sequences were obtained from the ^{1}H NMR spectrum. The Aib samples were dissolved in 700 μL of D_2O at a concentration of 0.04 M for ABA and BA_2 and 0.02 M for A_2B.

DFT Calculations. Some preliminary DFT calculations were carried out for the investigated peptides *in vacuo.* All calculations were carried out with the *TITAN* program, a joint product from Wavefunction, Inc. (Irvine, CA) and Schrödinger, Inc. (Portland, OR). The optimized geometries of the deuterated peptides (NH substituted by ND) were calculated at the B3LYP/6-31G** level for initial conditions specified below. Normal mode calculations were subsequently carried out for the thus obtained geometries.

Molecular Dynamics Simulations

Initial Conformations. The Ac-Aib-Ala-Ala-OMe, Ac-Ala-Ala-Aib-OMe, and Ac-Ala-Aib-Ala-OMe PDB files were created using Sybyl 7.3.[49] They were manually edited to satisfy the atom-name requirements of the pdb2gmx file-conversion program in GROMACS.[50,51] GROMACS topology files were manually appended to define the OMe residue and its torsion parameters. Four initial conformers were generated for each peptide sequence. The first conformer was a classical α-helix. Rotating the Aib φ torsion in the first conformer from −58° to +58° created the second conformer. The third and fourth conformers were classical β-strands except the Aib φ torsion was set to −58° or +58°, respectively. In total, 12 initial conformers were created (3 peptides × 4 conformers/peptide). Each peptide was solvated in a rhombic dodecahedron box of

(39) Brant, D. A.; Flory, P. J. *J. Am. Chem. Soc.* **1995**, *87*, 2791.
(40) Pappu, R. V.; Srinivasan, R.; Rose, G. D. *Proc. Natl. Acad. Sci. U.S.A.* **2000**, *97*, 12565.
(41) Carpino, L. A.; El-Faham, A.; Minor, C. A.; Albericio, F. *J. Chem. Soc., Chem. Commun.* **1994**, *1994*, 201−203.
(42) Schnölzer, M.; Alewood, P. F.; Jones, A.; Alewood, D.; Kent, S. B. H. *Int. J. Pept. Protein Res.* **1992**, *40*, 180−93.
(43) Alewood, P.; Alewood, D.; Miranda, L.; Love, S.; Meutermans, W.; Wilson, D. *Methods Enzymol.* **1997**, *289*, 14−29.
(44) Sarin, V. K.; Kent, S. B. H.; Tam J. P.; Merrifield, R. B. *Anal. Biochemistry* **1981**, *117*, 147−157.
(45) Sieler, G.; Schweitzer-Stenner, R. *J. Am. Chem. Soc.* **1997**, *119*, 1720.
(46) Measey, T.; Schweitzer-Stenner, R. *Chem. Phys. Lett.* **2005**, *408*, 123.
(47) Hagarman, A.; Measey, T.; Doddasomayajula, R. S.; Dragomir, S.; Eker, F.; Griebenow, K.; Schweitzer-Stenner, R. *J. Phys. Chem. B* **2006**, 110.
(48) Jentzen, W.; Unger, E.; Karvounis, G.; Shelnutt, J. A.; Dreybrodt, W.; Schweitzer-Stenner, R. *J. Phys. Chem.* **1996**, *100*, 14184.
(49) *Sybyl 7.3*; Tripos: St. Louis, MO, 2007.
(50) Lindahl, E.; Hess, B.; Van der Spoel, D. *J. Mol. Model.* **2001**, *7* (8), 306−317.
(51) Van Der Spoel, D. *J. Comput. Chem.* **2005**, *26* (16), 1701−18.

TIP4P water where the minimum distance between any peptide atom and the edge of the box was 10 Å for β-strand conformers and 13 Å for α-helices.[52] This resulted in approximately the same size box for both β-strand and α-helix conformations. The system was energy minimized, heated up to 300 K in 50 K increments where each increment was simulated for 20 ps at 1 fs timesteps. Production simulations (100 ns) were performed at 300 K using GROMACS. The constant number of molecules, pressure, and temperature (NPT) ensemble was used. Snapshots were recorded every 10 ps. Force field parameters were defined by the OPLS 2001 set.[53] Dihedral angles were calculated using the g-angle analysis program provided in the GROMACS package. The simulations were performed on local computing resources supplemented by the Teragrid supercomputer network.

Energy-Landscape Exploration. High-temperature (500 K) 30 ns simulations were performed to explore the energy landscape of each peptide sequence. The initial conformations of Ac-Aib-Ala-Ala-OMe, Ac-Ala-Ala-Aib-OMe, and Ac-Ala-Aib-Ala-OMe were linear where the φ and ψ torsions were set to $+180°$. The peptides were solvated, energy minimized, and simulated at 500 K for 30 ns. The NPT ensemble was used.

Analysis Tools. Phi, psi, and omega torsions were calculated for the 12 trajectories (3 peptide $\times$ 4 conformers/peptide). The atoms specific for each dihedral were manually identified and written to a file. Torsions from the first 3 ns of the simulations were excluded from the calculations. The g-angle program provided by GROMACS was used to calculate the angles. For each trajectory, the torsions of each amino acid in a peptide were binned into 90 $\times$ 90 squares, each covering an area of 4 $\times$ 4°.[54] The percentages of torsions that fall within a square were calculated. Squares with the highest percentages were colored coded dark-red, and squares with the lowest percentages were color-coded blue. White indicates that a square was not populated.

Results and Discussion

In this section of the paper, we first present the results of our spectroscopic experiments on Ac-Ala-Ala-Aib-OMe, Ac-Ala-Aib-Ala-OMe, and Ac-Aib-Ala-Ala-OMe and discuss them in qualitative terms. The second part describes the simulation of amide I′ band profiles in terms of different structural models. The results of this analysis are then compared with the respective ECD spectra. The last part describes the results of MD simulations from which the energy landscapes of the peptides were obtained.

Vibrational Spectra. Figures 1−3 show the amide I′ region of the IR, isotropic Raman, anisotropic Raman, and VCD spectra of Ac-Ala-Ala-Aib-OMe (Figure 1), Ac-Ala-Aib-Ala-OMe (Figure 2), and Ac-Aib-Ala-Ala-OMe (Figure 3) in D_2O. Using D_2O rather than H_2O eliminated vibrational mixing between solvent and amide I modes.[45,55] D_2O is known to slightly destabilize hydrogen bonds compared with H_2O,[56] but this just leads to a slight shift in equilibrium toward extended β-strands.[57] All profiles were highly asymmetric. For Ac-Ala-Ala-Aib-OMe and Ac-Ala-Aib-Ala-OMe (Figures 1 and 2), the first moment of the isotropic Raman profile was clearly at higher wavenumbers than that of the respective IR band. This noncoincidence is indicative of a predominant sampling of extended conformations in the upper left quadrant of the Ramachandran plot,[58,59] As recently demonstrated by Torii, a large negative noncoincidence ($\Omega_{IR}-\Omega_{iso} < -10$ cm^{-1}, Ω_{IR}: IR-peak position, Ω_{iso}: peak position of the isotropic Raman band) is indicative of a peptide predominantly sampling the PPII trough in the Ramachandran plot.[60] Ac-Aib-Ala-Ala-OMe, however, showed a different behavior in that the noncoincidence between IR, isotropic, and anisotropic Raman band peaks is substantially smaller than observed for the other two peptides. The peak position of the isotropic Raman band is downshifted and that of the IR-band upshifted compared with the respective positions in Ac-Ala-Aib-Ala-OMe and Ac-Ala-Ala-Aib-OMe. This could be indicative of a substantial sampling of either helical or turnlike structures[58,59] and of a shift of intrinsic amide I wavenumbers. The VCD spectra of Ac-Ala-Aib-Ala-OMe and Ac-Aib-Ala-Ala-Ala-OMe (Figures 2 and 3) both showed a purely negative signal, which were much less pronounced than the negative VCD band earlier observed for Ala_2-Lys-Ala and Ala_4.[36,37] The spectra were qualitatively different from the couplets observed for Ala_3.[61] The VCD spectrum of Ac-Ala-Ala-Aib-OMe (Figure 1) did not show a clearly discernible amide I signal.

Figure 4 exhibits the ECD spectra of the three peptides measured at different temperatures between 10 and 80 °C. At room temperature, their spectra all displayed a positive couplet, but their amplitudes and wavelength positions were different. We discuss these spectra in detail below.

Theoretical Concept for the Structure Analysis. The excitonic coupling model for amide I has been described in detail in several earlier papers.[62,59] The model describes the amide I band profiles of IR, isotropic Raman, anisotropic Raman, and VCD in terms of nearest neighbor and non-nearest neighbor excitonic coupling between the excited states of the local oscillators[63] and the dihedral angles ϕ and ψ of the residues between the interacting amide I modes. One counts the first central amide residue (starting at the N-terminal) as 1 and the subsequent one as 2. It should be noted that the C-terminal residue is not probed by the amide I′ band profile. Femtosecond two-dimensional IR spectroscopy has shown for cationic trialanine that vibrational coupling between the C-terminal carbonyl vibration and the adjacent amide I mode is negligibly small.[64] DFT calculations on Ac-Ala-Aib-Ala-OMe with deuterated amide groups *in vacuo* reveal some small coupling between the respective CO stretching vibration of the C-terminal ester group and the adjacent amide I′. The corresponding optimized geometry exhibits a PPII conformation for the first alanine, a right-handed 3_{10} for Aib, and an extended β-strand for the C-terminal alanine. This mixing is likely to be even weaker for the "real" peptide in aqueous solution since the

(52) Jorgensen, W. L.; Madura, J. D. *Mol. Phys.* **1985**, *56*, 1381−1392.
(53) Kaminski, G. A. *J. Phys. Chem. B* **2001**, *105* (28), 6474−6487.
(54) Hovmoller, S.; Zhou, T.; Ohlson, T. *Acta Crystallogr., Sect. D* **2002**, *58*, 768−76.
(55) Chen, X. G.; Schweitzer-Stenner, Asher, S. A.; Mirkin, N. G.; Krimm, S. *J. Phys. Chem.* **1995**, *99*, 3074.
(56) Shi, Z.; Olson, C. A.; Kallenbach, N. R.; Sosnick, T. R. *J. Am. Chem. Soc.* **2002**, *124* (13), 994−13 995.
(57) Eker, F.; Griebenow, K.; Schweitzer-Stenner, R. *J. Am. Chem. Soc.* **2003**, *125*, 8178−8185.
(58) Torii, H.; Tasumi, M. *J. Raman Spectrosc.* **1998**, *29*, 81−86.
(59) Schweitzer-Stenner, R. *J. Phys. Chem. B* **2004**, *108*, 16965.
(60) Torii, H. *J. Phys. Chem. B* **2007**, *111*, 5434.
(61) Eker, F.; Cao, X.; Nafie, L.; Schweitzer-Stenner, R. *J. Am. Chem. Soc.* **2002**, *124*, 14330.
(62) Schweitzer-Stenner, R. *Biophys. J.* **2002**, *83*, 523.
(63) Hamm, P.; Lim, M.; Hochstrasser, R. *J. Phys. Chem. B* **1998**, *102*, 6123.
(64) Woutersen, S.; Hamm, P. *J. Phys. Chem. B* **2000**, *104*, 11316−11320.

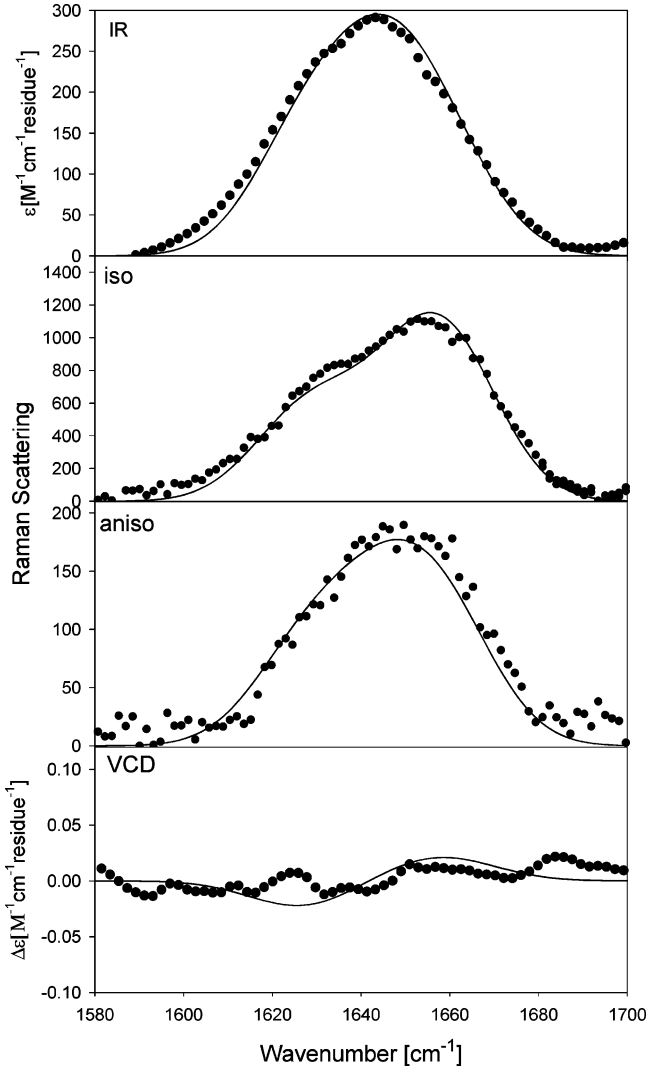

Figure 1. Amide I′ profiles (dotted) of the isotropic Raman, anisotropic Raman, IR, and VCD spectrum of Ac-AAB-OMe in D_2O. The solid line results from a simulation based on a multistate (per residue) model, encompassing a PPII, β-strand, and right- and left-handed 3_{10}-helix.

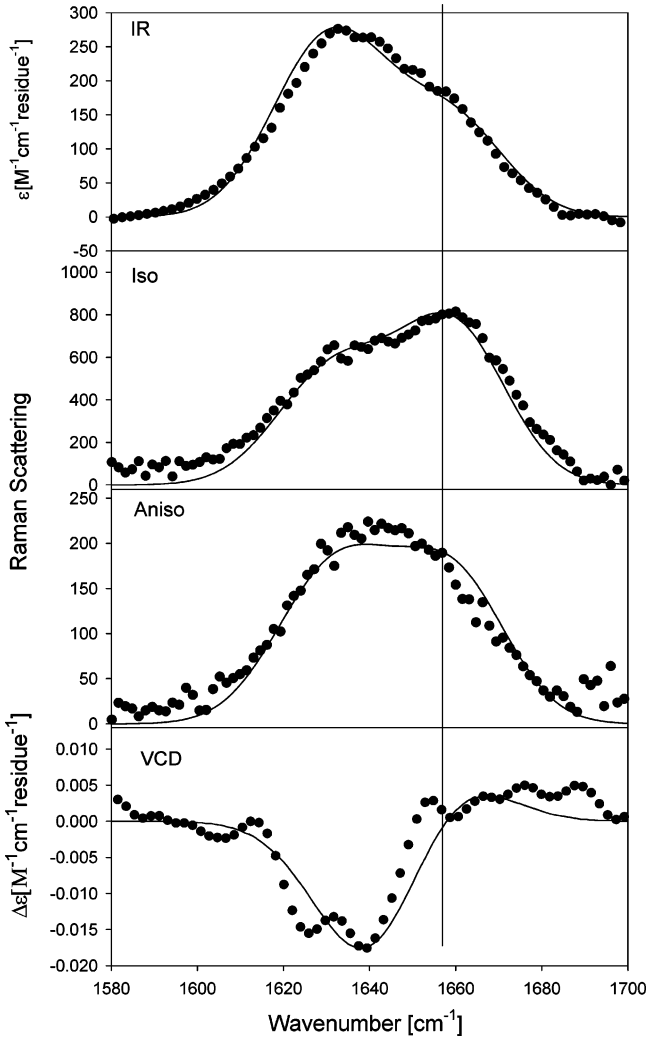

Figure 2. Amide I′ profiles (dotted) of the isotropic Raman, anisotropic Raman, IR, and VCD spectrum of Ac-Ala-Aib-Ala-OMe in D_2O. The solid line results from a simulation based on a multistate (per residue) model, encompassing a PPII, β-strand, and right- and left-handed 3_{10}-helix and a disordered type IV and IV′ β-turn.

experimentally obtained difference between the wavenumbers of the considered modes (72 cm^{-1}) is much larger than the theoretically predicted one (33 cm^{-1}).

Since each configuration of a peptide gives rise to an individual set of band profiles, the total intensity of a peptide ensemble is written as[37]

$$I(\Omega) = \frac{\sum_{i=1}^{3} \sum_{j_1,j_2=1}^{n_{c_1},n_{c_2}} (I_{ij_1j_2}(\Omega) \exp-(\sum_{k=1}^{n_{c_k}} G_{jk})/RT)}{Z} \qquad (2)$$

where G_{j_k} is the Gibbs energy of the k-th residue with the conformation j. The subscript i labels the excitonic state of the amide I′ oscillators. $I_{ij_1j_2}(\Omega)$ is thus the intensity profile of the *i-th* excitonic state associated with the configuration $\{j_1,j_2\}$ of the tetrapeptide. R is the gas constant, T is the absolute temperature, Z is the partition sum of the ensemble, and n_{c_1} and n_{c_2} are the number of conformations considered for the two central residues.

In our analysis, we considered five representative conformations, i.e., PPII ($j = 1$), β ($j = 2$), right-handed helical ($j = 3$), left-handed helical ($j = 4$), and type IV/IV′ β-turn ($j = 5,6$). The designation type IV normally encompasses a large variety of turn structures, which do not fit within the type I, II, III, and V category. In our case it solely represented conformation sampling in the bridge region between PPII and right-handed helical regions in the Ramachandran plot. Recent MD simulations by Bürgi et al.[30] suggested that Aib is able to adopt such conformations. The Gibbs energy of PPII was set to zero. Initially, we based our simulation on $(\phi,\psi)_1 = (-68°, 150°)$ and $(\phi,\psi)_2 = (-125°, 115°)$ for alanine, which represent respective distributions in the coil library of Avbelj and Baldwin[9] and correspond to the $^3J_{C\alpha HNH}$ constants reported by Shi et al.[65] Coil libraries as well as molecular dynamics simulations for alanine dipeptides generally exhibit helical distributions with a maximum at $(\phi,\psi)_3 = (-65°, -30°)$, which we assumed as representative for right-handed helical conformations.[10] These coordinates are closer to a 3_{10} than to a canonical α-helical

(65) Shi, Z.; Olson, C. A.; Rose, G. A.; Baldwin, R. L.; Kallenbach, N. R. *Proc. Natl. Acad. Sci. U.S.A.* **2005**, *102*, 17964.

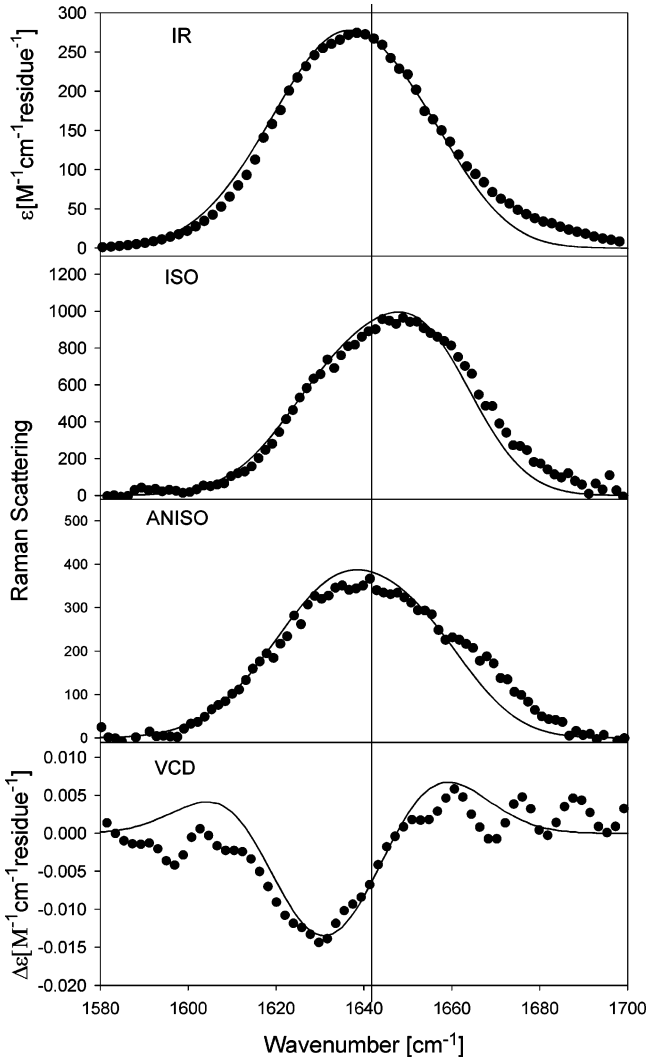

Figure 3. Amide I′ profiles (dotted) of the isotropic Raman, anisotropic Raman, IR, and VCD spectrum of Ac-Aib-Ala-Ala-OMe in D_2O. The solid line results from a simulation based on a multistate (per residue) model, encompassing a PPII, β-strand, and right- and left-handed 3_{10}-helix and a disordered type IV and IV′ β-turn.

conformation. In the following, we refer to this structural model as the "coil-library model." For Aib, we assumed the type III and III′ β-turn coordinates representing right-handed ($(\phi,\psi)_3 = (-60°, -30°)$) and left-handed ($(\phi,\psi)_4 = (60°, 30°)$) 3_{10}-like conformations. Alternatively, we considered the possibility that Aib samples predominantly α-helix-like conformations, which we represented by $(\phi,\psi)_3 = (-57°, -47°)$ (right-handed) and $(\phi,\psi)_4 = (57°, 47°)$ (left-handed). The type IV β-turn manifold was represented by $(\phi,\psi)_5 = (-60°, 10°)$, and the corresponding IV′ enantiomers were represented by $(\phi,\psi)_6 = (60°, -10°)$. This conformation could be described as a somewhat distorted C_7 conformation, which short alanine-based peptides can adopt in nonaqueous solutions.[66]

For the alanine residues, we used the $^3J_{C\alpha HNH}$ constants of the considered conformations obtained by employing a modified Karplus equation[67] with our experimentally determined coupling constants and determined the respective mole fraction of these conformations as follows:

$$\chi_{1,k} = \frac{[(J_k - J_{\beta,k}) - \chi_{3,k}(J_{\alpha r} - J_{\beta,k}) - \chi_{4,k}(J_{\alpha l} - J_{\beta,k})]}{J_{p,k} - J_{\beta,k}}$$

$$\chi_{2,k} = 1 - \chi_{1,k} - \chi_{3,k} - \chi_{4,k} \quad (3)$$

where $\chi_{j,k}$ is the mole fraction of the k-th residue in the j-th conformation, J_k is the measured coupling constant of the k-th residue, and $J_{p,k}$ and $J_{\beta,k}$ (4.8 and 9.8 Hz) are the coil-library coupling constants of the k-th residue for PPII and β as reported by Shi et al.[65] $J_{\alpha r} = 4.1$ Hz and $J_{\alpha l} = 7.0$ Hz are the representative coupling constant of the above right- and left-handed helical conformation, respectively. The experimentally determined $^3J_{C\alpha HNH}$ coupling constants of the respective alanine residues are listed in Table 1. The mole fraction $\chi_{3,k}$ and $\chi_{4,k}$ of these conformations have been used as an adjustable parameter in the simulation for alanine and Aib. For the latter, we additionally used $\chi_{5,k}$ and $\chi_{6,k}$ as free parameters. The mole fractions were used to calculate the relative Gibbs energies of the residues:

$$G_{j_k} = RT \ln\left[\frac{\chi_{j,k}}{\chi_{1,k}}\right] \quad (4)$$

that were used in eq 2 to calculate the intensity profiles.

Structure Analysis of Ac-Ala-Ala-Aib-OMe. Since the excitonic coupling depends solely on the dihedral angles of the residues between the amide I′ modes of interacting peptide bonds, the band profiles solely reflect the conformations of the two alanine residues. First, we needed estimated values for the intrinsic wavenumbers of the three coupled amide I′ vibrations in order to carry out the simulation of the band profiles. To this end a self-consistent spectral decomposition of Raman and IR band profiles was performed[61] that yielded the wavenumber values of three subbands listed in Table 2. We also measured the (IR) amide I band position for Ac-Ala-OMe in D_2O and obtained a value of 1629 cm^{-1}, which suggests that the 1628 cm^{-1} subband of Ac-Ala_2-Aib-OMe was assignable to the N-terminal peptide group. A comparison with the subbands of cationic and anionic tetraalanine[36] suggests that the band at 1661 cm^{-1} and 1646 cm^{-1} were assignable to the central and C-terminal peptide group, respectively. To calculate IR absorption and rotational strength (for VCD) in absolute units, the transition dipole moments of dialanine were used for all peptide groups.[68] The C-terminal amide I mode of small peptides generally exhibits some intrinsic rotational strength which is not due to the coupling with another oscillator. It most likely results from some electronic effect of the C-terminal carbonyl group.[36,61] In contrast to what was observed for Ac-Ala-OH, however, the amide I′ VCD signal of Ac-Aib-OH was very weak and barely discernible from noise (data not shown). The intrinsic contribution of the C-terminal Aib of Ac-Ala-Ala-Aib-OMe to the VCD band profile was, therefore, neglected. One would be tempted to check whether the data could be reproduced solely based on the crystal structure of Boc-Gly-Ala-Aib-OMe, a somewhat distorted type III β-turn. Indeed, this yielded a reasonable reproduction of Raman and IR band profiles but overestimated the VCD signal (data not shown). Moreover, this modeling was inconsistent with the $^3J_{C\alpha HNH}$ coupling constants

(66) Jalkanen, K. J.; Suhai, S. *Chem. Phys.* **1996**, *208*, 81.
(67) Vuister, G. W.; Bax, A. *J. Am. Chem. Soc.* **1993**, *115*, 7772.
(68) Measey, T.; Hagarman, A.; Eker, F.; Griebenow, K.; Schweitzer-Stenner, R. *J. Phys. Chem. B* **2005**, *109*, 8195.

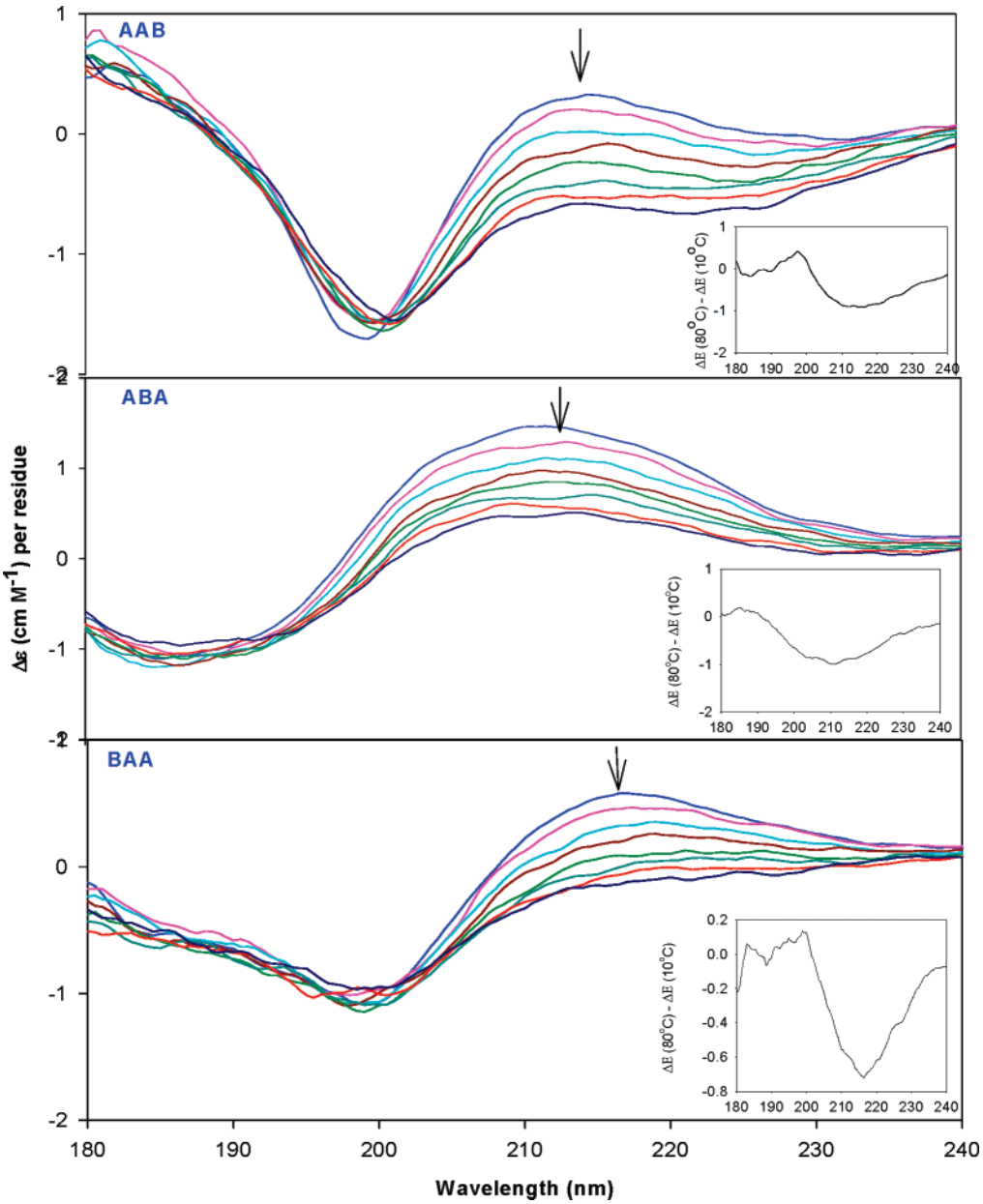

Figure 4. Temperature-dependent ECD spectra of Sc-Ala-Ala-Aib-OMe, Ac-Ala-Aib-Ala-OMe, and Ac-Aib-Ala-Ala-OMe measured from 10 to 80 °C in increments of 10 °C. The arrow indicates the change with increasing temperature. (Inset) Difference ECD spectrum obtained by subtracting the 10 °C from the 80 °C spectrum.

Table 1. $^3J_{C\alpha NH}$ Constant of Alanine Residues

	residue 1	residue 2
Ac-Aib-Ala−Ala-OMe		5.1 Hz
Ac-Ala-Aib-Ala-OMe	6.2 Hz	
Ac-Ala-Ala-Aib-OMe	5.5 Hz	5.5 Hz

Table 2. Wavenumbers of Three Subbands Obtained from a Self-Consistent Spectral Decomposition of the Amide I′ Band Profile

	Ac-Aib-Ala-Ala-OMe	Ac-Ala-Aib-Ala-OMe	Ac-Ala-Ala-Aib-Ome
Ω_1 [cm^{-1}]	1631	1626	1628
1659Ω_2 [cm^{-1}]	1649	1637	1646
Ω_3 [cm^{-1}]	1667	1659	1661

and also with the ECD spectrum in Figure 4, which was clearly indicative of a substantial PPII fraction at room temperature.

In a second attempt a three-state model for the two alanine residues was invoked, which was recently used to reproduce the amide I′ band profiles of short alanine-based peptides. It considers the coexistence of the aforementioned PPII ($j = 1$), β-strand ($j = 2$), and right-handed helix ($j = 3$).[37] It should be noted that only the molar fraction of the helical conformation was used as a free parameter. Thus, the simulated band profiles were close to the experimental ones, but we did not judge the agreement as satisfactory, particularly for VCD and anisotropic Raman spectra. This prompted us to allow for slight differences between the PPII coordinates of the alanine residues, as done earlier for tetraalanine.[36] The band profiles shown as solid lines in Figure 1 were produced with the PPII coordinates $(\phi,\psi)_1(j = 1) = (-63°, 150°)$ and $(\phi,\psi)_2(j = 1) = (-70°, 140°)$ that

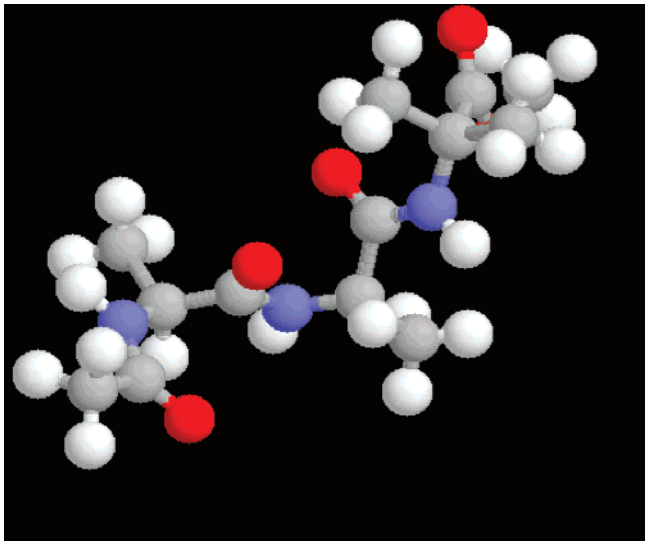

Figure 5. Structure of Ac-Ala-Ala-Aib-OMe with $(\phi,\psi)_1 = (\phi,\psi)_2 = (-60°, 150°)$ (PPII) and $(\phi,\psi)_3 = (-60°, -30°)$ (right-handed 3_{10}).

were only slightly different from canonical PPII-values.[69] We like to reiterate in this context that these conformations were representatives for distributions in the Ramachandran plot. We found that an addition of even small fractions of the helical conformation led to deterioration rather than improvement in the simulation spectra. The same conformational distribution was obtained for both residues, i.e., molar fractions of 0.78 for PPII and 0.22 for β-strand. This was indicative of a very pronounced PPII propensity of alanine and resembled the results obtained for cationic tetraalanine in D_2O.[36,38] Hence, we can conclude that the C-terminal Aib does not have a significant influence on the propensity of the two alanine residues. Figure 5 shows the most probable conformation with the sequence PPII-PPII-3_{10}. We assumed a right-handed 3_{10} conformation for Aib, but of course nothing can be said about which enantiomer was predominant. The weak VCD signal (compared with that of tetraalanine) can be explained by the substantial alkylation-induced downshift of the N-terminal amide I wavenumber (from ca. 1675 cm^{-1} in trialanine to 1628 cm^{-1} in Ac-Ala-Ala-Aib-OMe).

The ECD spectrum of the peptide was measured as a function of temperature as shown in Figure 4. The spectra taken at room temperature display a negatively biased couplet that is normally indicative of PPII.[70,71] However, both the negative and the positive signals were weaker than what was observed for tetraalanine, for which we obtained similar PPII fractions.[36,37] This is most likely due to the contribution of the C-terminal Aib, which can be expected to adopt a mixture of right- and left-handed helical conformations. As shown by Hagarman at al., the C-terminal residue of small peptides significantly contributes to the ECD signal, which most likely reflects coupling between the $\pi \rightarrow \pi^*$ transitions of the peptide groups and the C-terminal ester group.[47] Interestingly, the difference of the spectra taken at 80 °C and 10 °C shown in the inset of Figure 4 shows the typical minimum at 215 nm but does not display the strong positive signal at 195 nm observed for tri- and tetraalanine,[36,61] which together are indicative of an increased population of β-strand-like conformations. At 80 °C, the ECD spectrum shows two negative CD bands with a minimum above 220 nm. The high-temperature spectra clearly resemble what Drake et al. obtained when they measured the CD spectrum of poly-L-lysine in aqueous solution at neutral pH and high temperatures.[72] They interpreted their spectra as reflecting a mixture of PPII and helical conformations. Thus, it seems that contrary to expectation the alanine residues sample helical conformations at higher temperatures. The temperature dependence of $\Delta\epsilon$ at 215 nm is nearly linear, which rules out any involvement of cooperativity (data not shown).

Structure Analysis of Ac-Ala-Aib-Ala-OMe. The band profiles of this peptide are shown in Figure 2. The decomposition into three subbands assignable to individual peptide groups yielded the wavenumbers listed in Table 2. The band at 1626 cm^{-1} was again assigned to the N-terminal A. The highest wavenumber band results from the central peptide, and the central band was assignable to the C-terminal peptide. The $^3J_{C\alpha HNH}$ coupling constant of the N-terminal alanine was 6.1 Hz (Table 1), slightly higher than the corresponding value for Ac-A_2B-OMe, indicating a reduced PPII content. We used the recently observed intrinsic magnetic transition moments of amide I′ of neutral Ac-Ala for the C-terminal amide I′ mode.[37] As a first step, we assumed three conformations (PPII, β, right-handed helix) for alanine and a mixture of right-handed and left-handed helices for Aib. We performed simulations for both α- and 3_{10}-helices for different sets of molar fractions for the considered conformations but did not obtain a satisfactory agreement with all experimental profiles. All simulated spectra underestimated the intensity of the isotropic Raman band profile at low wavenumbers and the IR absorption at high wavenumbers. This led us to the conclusion that a conformation had to be considered for which the coupling constant between adjacent amide I modes was negative. The contour plot reported by Torii and Tasumi[58] suggests that this applies solely to conformations assignable to the bridge region connecting the PPII and helical troughs in the Ramachandran plot.[58] MD simulations of Aib-based peptides in DMSO by Bürgi et al. indeed suggested that Aib can sample this region and to a lesser extent also the corresponding enantiomers in the lower right quadrant of the Ramachandran plot.[30] This lead us to consider the aforementioned type IV/IV′ ($j = 5,6$) for the Aib-residue. The solid line in Figure 2 represents a simulation performed for the following molar fractions: $\chi_1 = 0.41$, $\chi_2 = 0.49$, and $\chi_3 = 0.1$ for the N-terminal alanine; $\chi_3 = 0.55$, $\chi_4 = 0.21$, $\chi_5 = 0.12$, and $\chi_6 = 0.11$ for Aib. A slightly modified 3_{10}-like conformation ($(\phi,\psi)_{1,2}(j = 3) = (-55°, -30°)$, $(\phi,\psi)_{1,2}(j = 4) = (55°, 30°)$ was assumed for conformations 3 and 4. The agreement with the experimental data was satisfactory. Replacing the two 3_{10} conformations by corresponding α-helical conformations led to deterioration of the quality of the IR and Raman profiles. It produces a W-shaped VCD signal with two negative and one positive band, not in agreement with the experimental data. We therefore conclude that 3_{10} was the preferred conformation for Aib in Ac-Ala-Aib-Ala-OMe. Figure 6 displays the structure of one of the dominant peptide sequences with PPII(Ala)-right-handed 3_{10}(Aib)-PPII.

Figure 4 exhibits the ECD spectrum of Ac-Ala-Aib-Ala-OMe measured between 10 and 80 °C. At 10 °C the couplet is rather

(69) Cowan, P. M.; McGavin, S. *Nature* **1955**, *176*, 501.
(70) Tiffany, M. L.; Krimm, S. *Biopolymers* **1968**, *6*, 137.
(71) Sreerama, N.; Woody, R. W. *Biochemistry* **1994**, *33*, 10022.
(72) Drake, A. F.; Siligardi, G.; Gibbons, W. A. *Biophys. Chem* **1988**, *31*, 143.

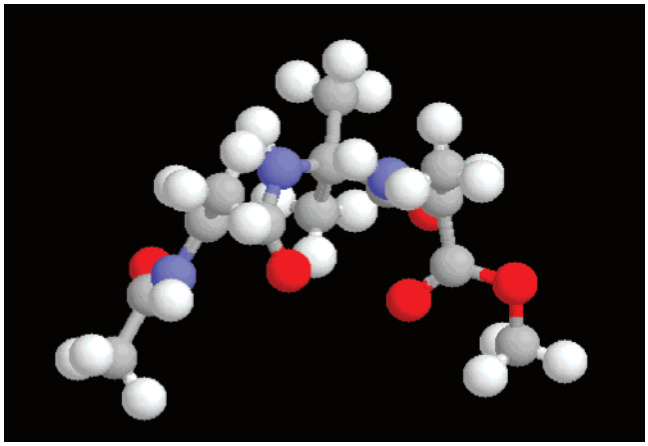

Figure 6. Structures of Ac-Ala-Aib-Ala-OMe with $(\phi,\psi)_1 = (-60°, 150°)$ (PPII), $(\phi,\psi)_2 = (-60°, -30°)$ (right handed 3_{10}), and $(\phi,\psi)_3 = (-60°, 150°)$ (PPII).

broad and symmetric thus deviating from the negatively biased canonical PPII signal.[70,71] Again, only the maximum decreased with increasing temperature, which gives rise to the broad minimum at 215 nm in the difference spectrum $\Delta\epsilon(80\ °C) - \Delta\epsilon(10\ °C)$ (inset of Figure 4). Generally, the observed spectrum is indicative of some type of left-handed turn. That would be in perfect agreement with the crystal structure of Ac-Ala-Aib-Ala-OMe[34] that exhibited both alanines in a PPII and the central Aib-residue in a left-handed 3_{10} conformation. Analysis of amide I′ profiles, however, yielded a surplus of right-handed 3_{10} for Aib. We performed simulations for different ratios of the two Aib enantiomeric conformers and found that even a modestly higher fraction of left-handed 3_{10} reduces the VCD signal significantly. If the left-handed conformation was predominant, the VCD spectrum would exhibit a positive Cotton effect. It should be noted in this context that a specific interpretation of the ECD spectrum is difficult in view of the fact that the C-terminal alanine, likely to adopt a mixture of PPII and β-strand, also contributes to the ECD signal.[47] Generally, ECD spectra are less of a local probe than VCD spectra. For short peptides they reflect electronic interactions between all π-electron moieties including the C-terminal carbonyl. Moreover, mixing with high energy $\sigma \rightarrow \sigma^*$ of side chains has been proposed to contribute to the spectrum in the 180−230 nm region.[73,74] In the case of Ac-Ala-Aib-Ala-OMe, the peptide adopted multiple conformations. If one considers the representative type IV turn also as left-handed, one obtains a fraction of nearly 0.2 for those peptides with all their residues adopting a left-handed conformation. Moreover, sequences with mixtures of residues adopting PPII, β, and right-handed 3_{10}, which account for a fraction of 39%, overall exhibit a left-handed helicity. The C-terminal Aib certainly samples the right- as well as the left-handed 3_{10}-trough of the Ramachandran plot. Hence, we concluded that the ECD spectrum did not contradict the result of our overall structure analysis.

The minimum at 190 nm maintained its strength and red-shifted with rising temperature. The positive CD band at 216 nm was concomitantly reduced. A comparison with the poly-L-lysine spectra measured by Drake et al. suggests a mixture of PPII, β-strand, and helical conformation for the alanine residues.[72] The contribution from the latter is certainly less pronounced than that in the spectrum of Ac-Ala-Ala-Aib-OMe. The temperature dependence of $\Delta\epsilon$ is less linear than that obtained for Ala-Ala-Aib but still not indicative of cooperativity (data not shown).

Structure Analysis of Ac-Aib-Ala-Ala-OMe. The band profiles of this peptide are shown in Figure 3. The decomposition into three subbands assignable to individual peptide groups yielded the wavenumbers listed in Table 2. The low wavenumber band at 1631 cm^{-1} was assigned to the N-terminal Aib, as suggested by the corresponding amide I′ wavenumber of Ac-Aib, i.e., 1629 cm^{-1}. The highest wavenumber band resulted again from the central peptide,[36] and the central band was assignable to the C-terminal amide. Again, we used the magnetic transition moment obtained for the amide I′ mode of Ac-Ala for the C-terminal amide I′ mode.[37] As argued below, however, these numbers did not reflect the complex composition of the band profile. The $^3J_{C\alpha HNH}$ coupling constant of the central alanine residue was 5.0 Hz (Table 1). This low value suggested either a substantial fraction of PPII or a significant population of a helical conformation.

The symmetry of the band profiles and the alignment of its peaks indicated that the peptide sampled predominantly helical conformations.[58,59] As a consequence, a simulation based on the assumption that the central alanine samples predominantly PPII with some admixture of β-strand and helical conformation[37,38] yielded band profiles quite distinct from the experimentally observed ones in Figure 3. None of the experimental band shapes and positions observed were reproduced. The band profiles in Figure 3 were then simulated by allowing various fractions of right-handed and left-handed helical conformations for the central alanine residue. However, none of these attempts were successful either, in that they all aligned the bands at significantly higher wavelengths than indicated by the experimental data. This is understandable since helical conformations are known to have their amide I intensities predominantly in the band associated with the in-phase combination of coupled oscillators.[58,59] In order to account for this discrepancy, we assumed that the intrinsic wavenumbers of the individual amide I′ modes shifted down if both residues Aib and Ala adopted either a right-handed or left-handed 3_{10} helical structure. These peptide conformations would be stabilized by hydrogen bonding between the N-terminal carbonyl and C-terminal amide group (cf. Figure 7 for the right handed conformation). A very satisfactory simulation shown in Figure 3 was eventually achieved by this procedure. The necessary wavenumber downshifts for peptides with both Aib and Ala in a right-handed 3_{10} conformation, were 20 cm^{-1} and 33 cm^{-1} for the terminal amide I′ modes and the central amide I′, respectively. Such a downshift of the intrinsic amide I wavenumber upon a PPII $\rightarrow$ 3_{10} transition can indeed be inferred from theoretical calculations of Woutersen et al.[75] For Aib, we obtained the molar fractions $\chi_3 = 0.45$, $\chi_4 = 0.35$, and $\chi_5 = 0.20$, whereas $\chi_1 = 0.14$, $\chi_2 = 0.06$, $\chi_3 = 0.6$, and $\chi_4 = 0.2$ were obtained for the central alanine residue. The molar fractions of the helical fractions of Aib were somewhat uncertain in that the inverse ratio still yields satisfactory simulations. In the framework of this model, however, it is clear that both enantiomers of Aib were substantially

(73) Woody, R. W. *J. Chem. Phys.* **1968**, *49*, 4797.
(74) Woody, R. W.; Seerama, N. *J. Chem. Phys.* **1999**, *111*, 2844.
(75) Woutersen, S.; Pfister, R.; Hamm, P.; Mu, Y.; Kosov, D. S.; Stock, G. *J. Chem. Phys.* **2002**, *117*, 6833.

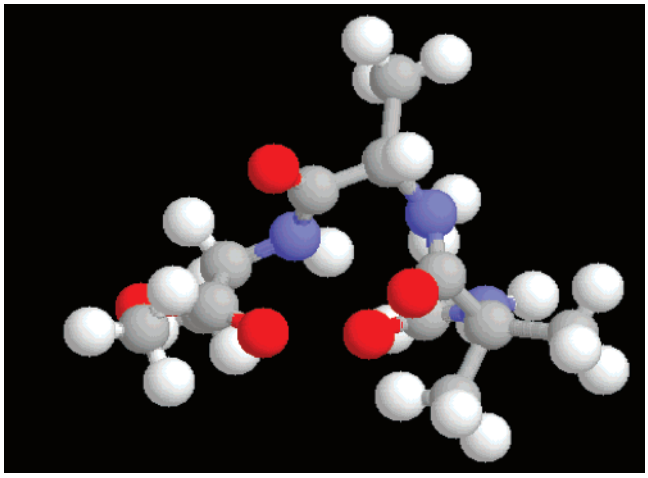

Figure 7. Structures of Ac-Aib-Ala-Aib-OMe with (a) $(\phi,\psi)_1 = (-60°, -30°)$, $(\phi,\psi)_3 = (-60°, -30°)$ (both right-handed 3_{10}), and $(\phi,\psi)_3 = (-60°, 150°)$ (PPII).

populated. We tried the same simulation based on the assumption that the residues adopt α_R rather than 3_{10}, but this did not reproduce the VCD signal and the agreement with IR and Raman profiles was less satisfactory.

Being concerned by the large number of parameter changes we had to invoke for the satisfactory simulations shown in Figure 3, we tried a more simplistic model by assuming that even in the absence of an overall helical structure the wavenumber of the amide I′ mode of the central peptide group was downshifted due to the fact that Aib adopted a helical conformation. Thus, we obtained a satisfactory reproduction of the Raman and IR band profiles for a -24 cm^{-1} shift and slight adjustments for the wavenumbers of the terminal amide I′ modes. The VCD signal, however, was less well reproduced. The corresponding molar fractions for alanine were $\chi_1 = 0.62$, $\chi_2 = 0.13$, $\chi_3 = 0.2$, and $\chi_4 = 0.05$. We would not totally dismiss this model just based on the somewhat less satisfactory agreement with the experimental data because of the smaller number of adjustable parameters. However, if we did not invoke an overall helical conformation of the peptide it is difficult to understand why Aib would *per se* influence the amide I′ mode only in Ac-Aib-Ala-Ala-OMe, but not in Ac-Ala-Aib-Ala-OMe, for which our data (i.e., the measured band profiles) rule out this possibility.

In order to search for further evidence in support of the assumed influence of the residue conformation on the intrinsic amide I wavenumber we carried out normal mode calculations for Ac-Ala-Aib-Ala-OMe and Ac-Aib-Ala-Ala-OMe *in vacuo* based on a DFT calculation using the B3LYP /6-31G** level. The initial dihedral angles chosen for the geometry optimization exhibited $(\phi,\psi)_N = (-60°, 150°)$, $(\phi,\psi)_{Ce} = (-60°, -30°)$, and $(\phi,\psi)_C = (-60°, 150°)$ for Ac-Ala-Aib-Ala-OMe and $(\phi,\psi)_N = (-60°, -30°)$, $(\phi,\psi)_{Ce} = (-60°, -30°)$, and $(\phi,\psi)_C = (-60°, 150°)$ for Ac-Aib-Ala-Ala-OMe (N: N-terminal, Ce: central residue, C: C-terminal) The optimization process yielded backbone conformations with $(\phi,\psi)_N = (-81°, 90°)$, $(\phi,\psi)_{Ce} = (-59°, -34°)$, and $(\phi,\psi)_C = (-151°, 178°)$ for Ac-Ala-Aib-Ala-OMe and $(\phi,\psi)_N = (-62°, -33°)$, $(\phi,\psi)_{Ce} = (-85°, 0°)$, and $(\phi,\psi)_C = (-98°, 80°)$. Since we did not consider solvation, these are not exactly the conformations we derived from our experimental data, but the conformation of the central alanine in Ac-Aib-Ala-Ala-OMe is close enough to the helical trough in the Ramachandran plot to ensure that a comparison of the amide I wavenumbers is at least of qualitative relevance. The vibrational analysis yielded substantial vibrational coupling between the amide I′ modes for both peptides investigated. Compared with Ac-Ala-Aib-Ala-OMe, the wavenumbers of the amide I′ vibrations mostly associated with the central and the C-terminal residues of Ac-Aib-Ala-Ala-OMe are reduced by 10 cm^{-1}, whereas the amide I′ of the N-terminal residue shifts up by 19 cm^{-1}. The latter certainly result from intrapeptide hydrogen bonding between the CO of residue 1 and the C-terminal amide group. In aqueous solution the situation would be different owing to additional hydrogen bonding to H_2O, which generally causes a substantial amide I downshift.[76] Altogether, these results qualitatively support the assumption we made regarding the intrinsic amide I′ wavenumbers of Ac-Aib-Ala-Ala-OMe.

An initial inspection of the room-temperature ECD spectrum in Figure 4 reveals a weak PPII signal. However its minimum appears at 200 nm that would be characteristic of a left-handed turn. Moreover, this minimum did not shift or decrease with increasing temperature, which would not be expected if it reflected a PPII conversion to β-strand. The difference spectrum $\Delta\epsilon(80\ °C) - \Delta\epsilon(10\ °C)$ (inset of Figure 4) shows a rather large minimum at 216 nm (-0.8 M^{-1} cm^{-1} per residue), which is again not accompanied by a maximum below 200 nm. It could be indicative of a right-handed 3_{10}-helix, but the (room temperature) maximum at 215 nm clearly reflects some left-handed turn or PPII conformation. It decreased with increasing temperature, and a comparison with the poly-L-lysine spectra of Drake et al. suggests again a mixture of PPII, β-strand, and helical conformation.[72] It is arguable that a mixture of right-handed, left-handed, and mixed structures could give rise to the observed ECD spectrum at room temperature. In this context, we have to recall again the contribution of the C-terminal alanine whose structural behavior could not be explored. The temperature dependence of $\Delta\epsilon$ departs from linearity above 50 °C (data not shown), but the statistical errors of the data points are too large to allow any conclusions concerning cooperativity.

Energy-Landscape Exploration. High-temperature simulations can cross energy barriers and provide accurate estimates of the energy landscape of peptide sequences.[77,78] Simulations of Ac-Aib-Ala-Ala-OMe, Ac-Ala-Aib-Ala-OMe, and Ac-Ala-Ala-Aib-OMe at 500 K showed that Aib samples both the right- and left-handed α-helix areas of the Ramachandran plot (Figure 8). The alanine residues sample a much larger region compared to Aib. While the φ angles of the alanine residues are mostly limited to the $-180°$ to $-60°$ region, the ψ angles sample the entire region between $-180°$ and 180°. Some alanine conformations also sampled the 60° phi region.

To determine if simulations at 300 K could sufficiently sample the estimated landscape at 500 K, we performed five 30 ns simulations of Ac-Aib-Ala-Ala-OMe where the initial conformers were 3_{10}-helix, α-helix, β-strand, linear strand, and a structure with random torsion angles. These 300 K simulations showed that the energy barrier for Aib between the right-handed helix ($\varphi = -65°$, $\psi = -45°$) and the left-handed helix ($\varphi = 65°$, $\psi = 45°$) regions was too high to be sampled within the

(76) Williams, S.; Causgrove, T. P., Gilmanshin, R.; Fang, K. S.; Callender, R. H.; Woodruff, W. H.; Dyer, R. B. *Biochemistry* **1996**, *35*, 691.
(77) Day, R. *J. Mol. Biol*. **2002**, *322* (1), 189−203.
(78) Li, A.; Daggett, V. *Proc. Natl. Acad. Sci. U.S.A.* **1994**, *91* (22), 100−4.

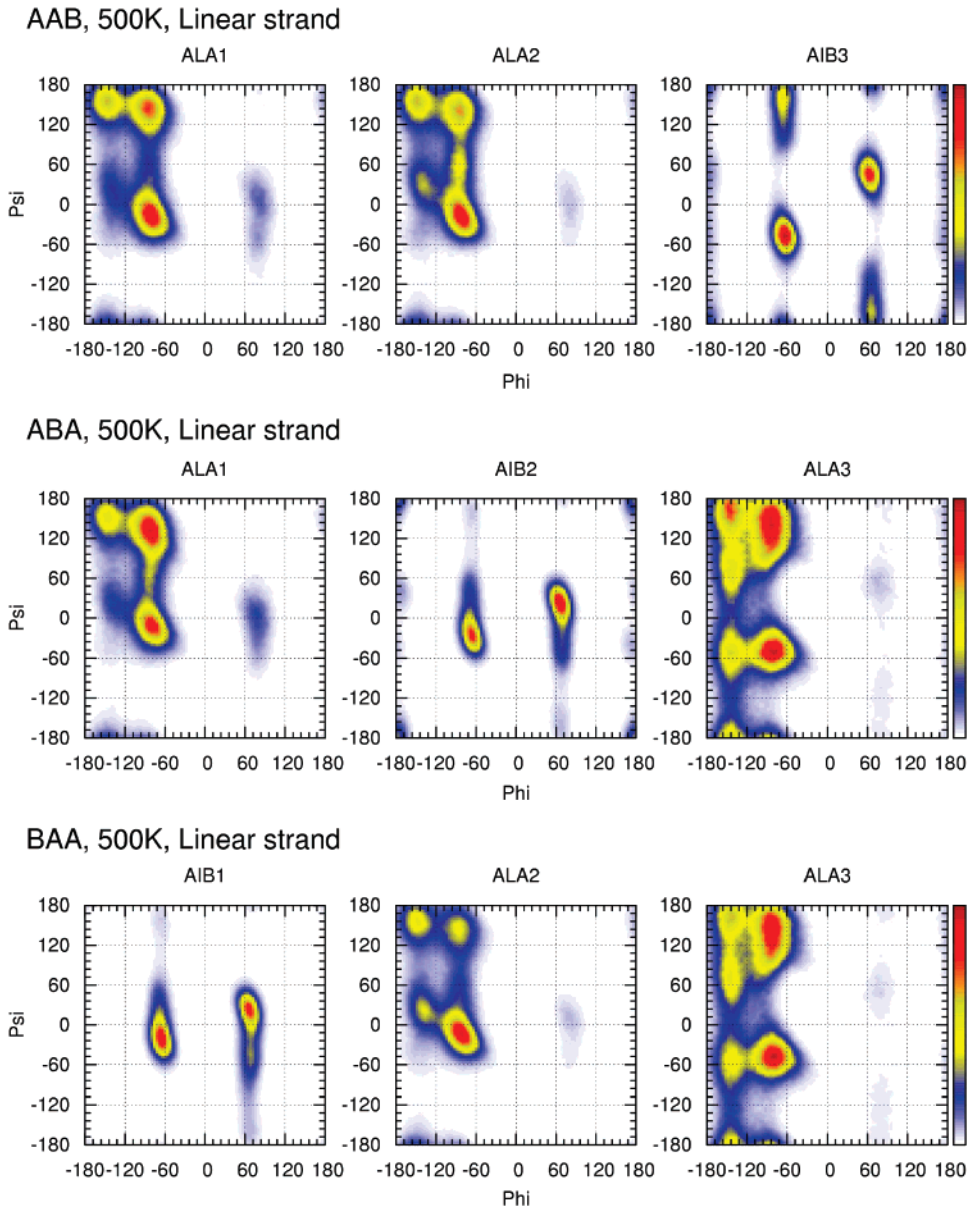

Figure 8. Ramachandran plots of Ac-Ala-Ala-Aib-OMe, Ac-Ala-Aib-Ala-OMe, and Ac-Aib-Ala-Ala-OMe snapshots from 30 ns, 500 K simulations. The initial structures were linear peptides with φ, ψ, and ω torsions set to 180°. Red indicates the highest percentage of the population, and white indicates that a region was not populated.

simulation time scale (data not shown). The alanine residues were able to sample the same regions as those found at 500 K. The barrier for Aib between helical regions was much higher than that of alanine due to Aib's extra methyl group on the α-carbon. Because of this limitation, it was necessary to seed the Aib φ torsion of the initial conformers to 58° or −58° in separate simulations. Seeding the torsions forced the Aib residue to sample either the right-handed or left-handed helical region, while the alanine residues sampled the allowed regions of the Ramachandran plot.

Transition Pathway between Right- and Left-Handed Helical Regions. During the 500 K simulations, Aib underwent transitions between left-handed and the right-handed helical regions. The φ torsion of Aib was mostly limited to the ±60° region, but it also explored the ±180° region. The ψ torsion, on the other hand, rotated more freely in all three peptide sequences (Figure 8). The reaction pathways for transitions from the left-handed helical region to the right-handed helical region were mapped for the Ac-ABA-OMe sequence. Figure 9 shows the φ torsion of Aib as it moves from the lower energy 60° state to the higher energy 180° intermediate state. Snapshots were recorded every 50 fs to capture the short-lived transitional conformers. Four snapshots spanning 200 fs were observed during the transition. From the 180° intermediate state, Aib can fall into either the left- or right-handed helical conformations. Two transition pathways were layered on top of a potential energy contour plot of acetyl-aminoisobutyric *N*-methylamide (Ac-Aib-NMA) (Figure 10). The potential energy contour plot was generated by systematically scanning the φ and ψ torsions of Aib in Ac-B-NMA followed by energy minimization in an implicit solvent (GB/SA). Transition A in Figure 10 shows a pathway taken by Aib as its φ transitions from 60° to ±180° to −60°. It starts at an energy minimum in the left-handed helix regions (60°, 30°) and climbs over the lowest-energy barrier (approximately 3.5 kcal/mol) (120°, −20°) to reach the intermediate states at $\varphi = \pm 180°$. From the intermediate state, Aib

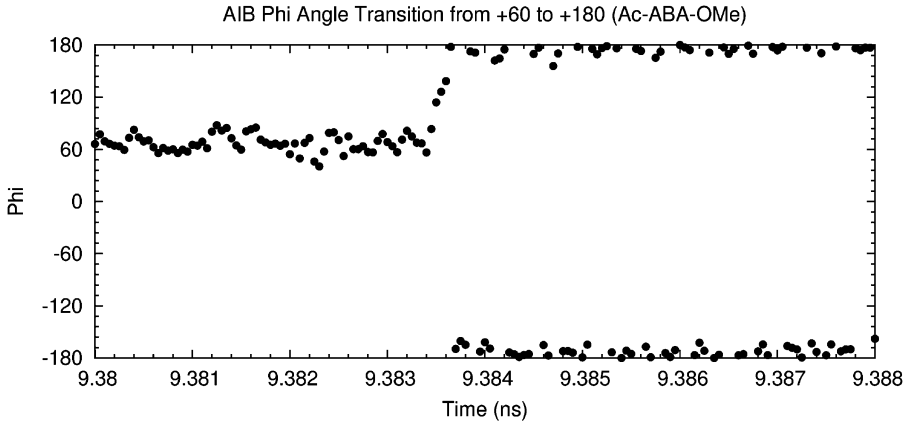

Figure 9. Change of Aib Ψ torsion angle in Ac-Ala-Aib-Ala-OMe during a concerted transition between right- and left-handed helical conformers of Aib residue at time 9.384 ns during a 30 ns 500 K Ac-Ala-Aib-Ala-OMe simulation. The φ angle moved from the left-handed helix torsion of 60 to the higher energy torsion at ±180.

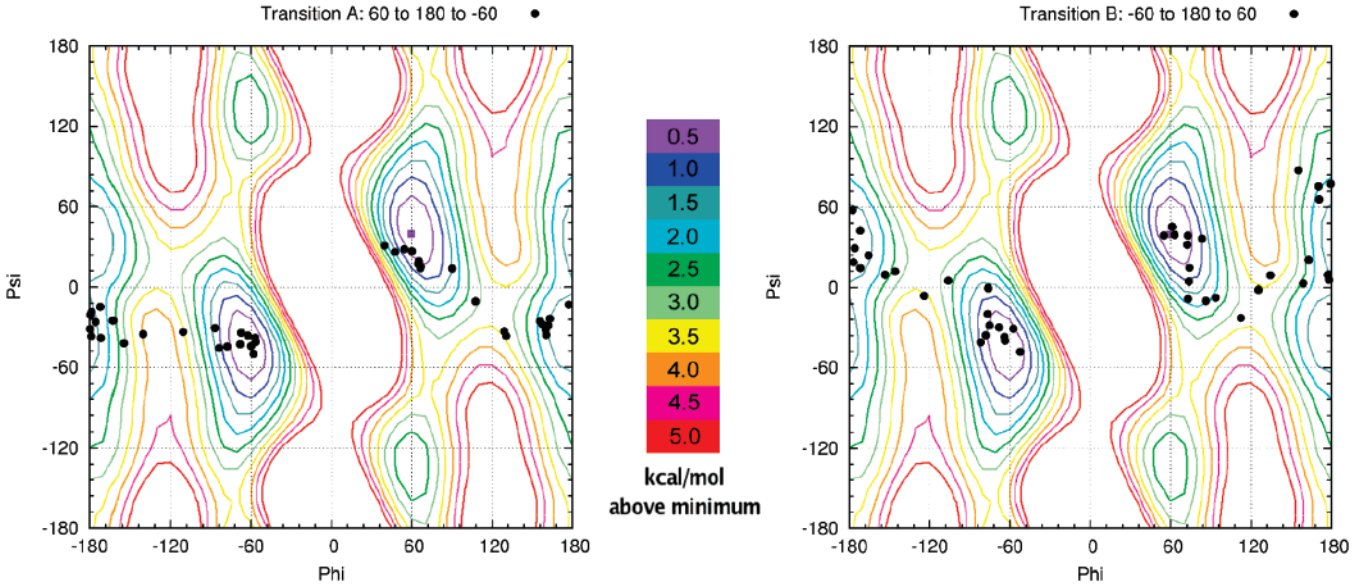

Figure 10. Pathways in Aib Φ,Ψ-space for transitions between right- and left-handed helical conformers of the Aib residue in Ac-Ala-Aib-Ala-OMe. Pathways A (Φ = 60 to ± 180 to −60) and B (Φ = −60 to ± 180 to 60) are layered on top of a potential energy contour plot of Ac-Aib-NMA. Each ● represent an Aib conformation as it undergoes a transition between two states.

climbs over an energy barrier that is approximately 4.0 kcal/mol (0.5 kcal/mol higher than the lowest-energy barrier) to reach the right-handed helix region (−60°, 30°). Two transitions from 180° to −60° show Aib climbing over the lowest-energy barrier (approximately 3.5 kcal/mol) to reach the (−60°, 15°) region (data not shown). Transition B in Figure 10 shows a pathway taken by Aib as its φ moves from −60° to ±180° to 60°. It starts at the right-handed helical region (−60°, −30°) and climbs over the lowest-energy barrier (3.5 kcal/mol) (−120°, 20°) to reach the intermediate states at (±180°, 30°). From the intermediate state, Aib climbs over an energy barrier at (120°, −20°) to reach the left-handed helix region (60°, 30°). The ψ angles range mostly from −60° to 60° in the transition pathways shown in Figure 10. The ψ angles in other pathways stay between 120° and 180° as the φ angle rotates from 60° to ±180° to −60° (data not shown). The potential energy plot of Aib in Figure 10 shows an accessible pathway for ψ to rotate between ±60° to ±180°. When the ψ angle is between 120° and 180°, the energy barrier for φ to rotate from 60° to 180° is higher than 5.0 kcal/mol.

All observed φ angle transitions between 60° and −60° pass through an intermediate state for φ as φ increased towards ±180°. A φ value of zero was not observed in any of the three 500 K peptide simulations. The potential energy profile of Ac-Aib-NMA indeed showed a lowest-energy path between the two α-helical regions through the ±180 region of φ (Figure 10). Similar to our 500 K simulation, the potential energy surface surrounding the φ = 0 region was too high to be plausibly explored.

300 K Simulations. The most populated regions of the Ramachandran plot of each residue in the three sequences are listed in Table 3. Their respective Ramachandran plots are shown in Figures S1 to S3 in the Supporting Information. The results for all three peptides were independent of whether the initial conformation was an α-helix or a β-strand. The φ angle of Aib impacted the neighboring amino acids' conformational preference for all three sequences with Ac-Aib-Ala-Ala-OMe showing the largest differences.

Table 3 lists the center of the most populated regions of the Ramachandran plot for the three peptides. Listed in column A

Table 3. Phi and Psi Torsions of Individual Residues in the Three Peptide Sequences[a]

	A: α-helix $\Phi_B = -58$			B: β-strand $\Phi_B = -58$			C: α-helix $\Phi_B = +58$			D: β-strand $\Phi_B = +58$		
	res 1	res 2	res 3	res 1	res 2	res 3	res 1	res 2	res 3	res 1	res 2	res 3
Ala-Ala-Aib	−80, 150 −80, −25	−80, 150 −80, −30	−65, −45 −65, 155	−80, 150 −80, −25	−80, 145 −80, −30	−65, −45 −65, 155	−80, 150 −80, −25	−80, 145 −75, −25	65, 45 65, −165	−80, 150 −80, −25	−80, 145 −80, −25	65, 45 65, −165
Ala-Aib-Ala	−80, 140 −75, −15	−65, −30	−80, −50 −80, 120	−80, 140 −75, −15	−65, −30	−80, −50 −80, 120	−75, 130 −80, −20	65, 25	−80, 130 −80, −45	−75, 130 −80, −20	65, 25	−80, 130 −80, −45
Aib-Ala-Ala	−65, −25	−80, −20 −140, 20 −80, 150 −140, 155	−80, 130 −80, −50 −140, 60	−65, −25	−80, −20 −140, 20 −80, 150 −140, 155	−80, 130 −80, −50 −140, 60	65, 30	−80, 150 −80, −25 −150, 160	−80, 130 −80, −50	65,30	−80, 150 −80, −25 −150, 160	−80, 130 −80, −50

[a] The conformations of the initial structures are indicated by the top row. $\Phi_B = -58$ indicates that the phi torsion of Aib was set to −58 in the initial conformation. The backbone torsions are listed in (φ,ψ) pairs with the most populated region placed on top of each box.

are the $\varphi-\psi$ torsions of the three peptides where the initial conformer for the simulations were α-helices. Listed in column B are the torsions where the initial conformers were β-strands except that the φ torsion of Aib was set to −58°. Listed in columns C and D are torsions where the φ torsion of Aib was set to +58° and the rest of the residues were either α-helices (C) or β-strands (D). When the initial φ torsion of Aib was set to −58°, results for the three peptides where the initial conformer was an α-helix (A) were nearly identical to those where the initial conformer was a β-strand (B). Similarly, when the initial φ torsion of Aib was set to +58°, results for the three peptides were nearly identical regardless of the conformations of the initial structures. This suggests that the simulations had converged. While the simulation results were nearly identical when the φ torsion of Aib was set to either −58° or +58°, the alanine conformations depended on the initial handedness of the Aib residue. The degree of dependency was greatest for Ac-Aib-Ala-Ala-OMe.

Ac-Ala-Ala-Aib-OMe. Ala_1 mainly populated the two regions at (−80°, 150°) and (−80°, −25°), but some conformations also explored the (−150°, 160°) region (Figure S1). Ala_1 conformation was not influenced by the initial handedness of Aib_3. The conformation of Ala_2, however, was slightly dependent on the initial φ torsion of Aib_3. When the φ torsion of Aib_3 was centered at +65°, the ψ torsion of Ala_2 shifted toward the region at 145°, increasing its polyproline II population. Like Ala_1, Ala_2 also explored the (−150°, 160°) region of the Ramachandran plot. There was also a small population centered at (−140°, 30°). Aib_3 mainly populated the (−65°, −45°) and (65°, 45°) region, corresponding to the right-handed and left-handed helix, respectively. Two smaller regions at (−65°, 165°) and (65°, −165°) were also populated. The φ torsion was more flexible because Aib_3 was at the C-terminus, and there was no additional amino acid side chain to restrict its rotation. The most populated regions explored by the 500 K simulation were also explored by the four 300 K simulations indicating that all low energy conformations were well sampled in the four 300 K simulations.

The results of the above simulations are apparently in good agreement with the peptide's structural manifold inferred from the amide I′ band profile of Ac-Ala-Ala-Aib-OMe in that both indicate that PPII is the predominant conformation sampled by the two alanine residues. This agrees well with multiple experiments and with coil libraries which all suggest a high PPII propensity of alanine.[36,37,79] A discrepancy exists concerning the occupancy of the less populated β-strand and 3_{10} helix. The best simulation of the amide I′ profiles were observed by confining ourselves to PII and β-strand, for which we obtained molar fractions of 0.78 and 0.22, respectively. The results of the MD simulations, however, indicate a significant sampling of (right-handed) helical conformations. We performed simulations for different mole fractions of a representative right-handed 3_{10}-helix and found that the simulations deviate substantially from the experimental profile for helical fractions above 0.1. It should be mentioned in this context that MD simulations based on a variety of force fields generally overestimate the sampling of helical conformations for alanine.[80−82]

Ac-Ala-Aib-Ala-OMe. When the Aib_2 torsions were centered at (65°, 25°), the majority of Ala_1 conformations were centered at (−75°, 130°) (Figure S2). A small percentage of conformations occupied the (−80°, −20°) helical region. When Aib_2 torsions were centered at (−65°, −30°), Ala_1 populated the (−80°, 140°) and (−75°, −15°) regions of the Ramachandran plot. Aib induces a higher percentage of Ala_1 helical conformations when its φ and ψ were centered at the (−65°, −30°) region. Ala_1 conformation depended on the handedness of Aib_2. Ala_3 conformations populated the (−80°, 120°) and (−80°, −50°) regions and were less dependent on Aib handedness. The population shifted toward the (−80°, −50°) region when the Aib_2 torsions were centered at (−65°, −30°). Similar to Ac-Ala−Ala-Aib-OMe, the most populated regions explored by the 500 °K simulation were also explored by the four independent 300 °K simulations.

The results of these simulations are in excellent agreement with the structural models used for the simulation of the corresponding amide I′ profiles. For the central Aib, sampling of both helical enantiomers is suggested by theory and experiment. For the N-terminal alanine, PPII is clearly the dominant conformation with some sampling of helical and β-strand conformations. Apparently, the extent to which these conformations are sampled depends on the initial conditions of the simulation (Figure S2). In accordance with Bürgi et al.[30] we obtained some minor sampling of the (type IV) bridge region slightly above $\psi = 0°$, which again agrees at least qualitatively with what we inferred from the spectroscopic data.

(79) Shi, Z.; Cheng, K.; Liu, Z.; Ng, A.; Bracken, W. C.; Kallenbach, N. R. *Proc. Natl. Acad. Sci. U.S.A.* **2005**, *102*, 17964.
(80) Duan, Y.; Wu, C.; Chowdhury, S.; Lee, M. C.; Xiong, G.; Zhang, W.; Yang, R.; Cieplak, P.; Luo, R.; Lee, T.; Caldwell, J.; Wang, J.; Kollman, P. *J. Comput. Chem.* **1999**, *24*, 1999.
(81) Gnanakaran, S.; Garcia, A. *J. Phys. Chem. B* **2003**, *107*, 12555.
(82) Zagrovic, B.; Lipfert, J.; Sorin, E. J.; Millett, I. S.; Van Gunsteren, W. F.; Doniach, S.; Pande, V. S. *Proc. Natl. Acad. Sci. U.S.A.* **2005**, *102*, 11698.

Ac-Aib-Ala-Ala-OMe. Among the three peptide sequences examined, Ac-Aib-Ala-Ala-OMe showed the strongest dependency on Aib handedness. Thus, the MD simulations strongly corroborate the results from our amide I′ analysis. Mainly, Ala_2 conformations changed dramatically when Aib_1's conformation moved from the (−65°, −25°) region to the (65°, 30°) region (Figure S3). On the other hand, Ala_3 conformations were much less sensitive to Aib_1 handedness and mainly populated the (−80°, 130°) and (−80°, −50°) regions of the Ramachandran plot. When Aib_1 torsions were centered at (−65°, −25°), Ala_2 populated four regions located at (−80°, −20°), (−140°, 20°), (−80°, 150°), and (−140°, 155°). When Aib_1 was in the (65°, 30°) region, A_2 populated mainly three regions located at (−80°, 150°), (−80°, −25°), and (−150°, 160°). The major differences between these two sets of Ala_2 conformations were the disappearance of the (−140°, 20°) region and the significant increase in population at (−80°, 150°) when A_2 changed from right-handed helix (−65°, −25°) to left-handed helix (65°, 30°). Similar to the cases for Ac-Ala-Ala-Aib-OMe and Ac-Ala-Aib-Ala-OMe, the most populated regions explored by the 500 K simulation were also explored by the four independent 300 K simulations.

Conclusions and comparison with Literature. The crystal structure of Ac-Ala-Aib-Ala-OMe and Boc-Gly-Ala-Aib-OMe have been determined by Jung and associates.[33−35] For the former the authors derived a new type of β-turn stabilized by a very weak 4 → 1 hydrogen bond.[34] While the two alanine residues adopt a clear PPII conformation, the Aib residue exhibited a slightly distorted left-handed 3_{10} or type III β-turn conformation. Our results indicate that the peptide adopts multiple conformations in solution. For the N-terminal alanine residue, PPII, β-strand and to a minor extent right-handed 3_{10} conformations coexist. The PPII propensity was slightly less than that observed for the central residue of trialanine.[61] For Aib the experimental data indicate some preference for a right-handed 3_{10}-like helical structure and additional sampling of the bridge region connecting the PPII and helix region on the right- and left-hand side of the Ramachandran plot. This was in full agreement with results from MD simulations of an Aib-rich peptide in DMSO.[30] Our MD simulations suggest that both right- and left-handed helical conformations are sampled.

The crystal structure of Ac-Gly-Ala-Aib-OMe, which one might regard as a good model for Ac-Ala_2-Aib-OMe, showed a somewhat deformed type III β-turn conformation with the glycine and alanine residues in right-handed 3_{10} conformations.[33] This is definitely not the solution structure. We found that in Ac-Ala_2-Aib-OMe both alanine residues behave just as they do in (cationic) tetraalanine.[36,37,60] They exhibit a rather high PPII propensity with some admixture of β-strand. This shows that the C-terminal Aib does not have a detectable influence on residues on its N-terminal side. Altogether, the comparison of crystal and solution structure revealed that the former might be of limited use for understanding the structural properties in solution, since lattice forces apparently select and stabilize particular peptide conformations in the crystal. Bosch et al. made an opposite claim for Boc-Ala-Aib-Ala-OMe in methanol, but we doubt that their results from ^{1}H NMR and ECD were sufficient for assessing the solution structure.[33]

The consistent results obtained from spectroscopy and MD simulations for Ac-Aib-Ala-Ala-OMe provide conclusive evidence for the notion that the N-terminal Aib, for which we obtained a mixture of right-handed and left-handed 3_{10}-helices, imposes a helical conformation on its nearest neighbor. This is indicative of a break down of the isolated pair hypothesis, which solely considers the two peptide neighbors of a given residue as relevant for local interactions. Pappu et al. performed simulations for an alanine polypeptide and found that non-nearest neighbor interactions have to be taken into account if a residue samples the helical region.[40] That might apply even more to Aib since it has been shown to substantially increase the thermostability of peptides and proteins. This has been attributed to the fact that its conformational space is not much increased in the unfolded state, so that a substitution of, e.g., alanine with Aib reduces the entropy difference between folded and unfolded states.[15] Our results suggest that this entropy reduction extends to the next neighbor toward the C-terminus.

The number of studies on peptides with Aib residues in aqueous solution is rather limited. Since Aib is often incorporated into peptides with a high hydrophobic content, the crystalline state or organic solvents are generally observed experimentally.[14,15,19,21,83,84] One of the few comprehensive experimental studies using water as solvent was carried out by Schievano et al.[29] who studied a series of Ac(Asn-Aib-Aib-Lys)$_n$Ala-OH ($n = 1, 2, 3$) peptides in water in SDS-containing micelles. Their NMR data led them to conclude that a 3_{10}-helix was adopted for dimers ($n = 2$) and trimers ($n = 3$). NMR and ECD data suggested an increase of 3_{10}-helix formation upon chain elongation. For $n = 1$ their ECD data suggest a PPII-like conformation, but that is certainly not the case for Aib-residues. Thus, their data were not indicative of the capability of short Aib-containing peptides to form a helix-like turn in solution.

Reaction pathways that allow Aib in Ac-Ala-Aib-Ala-OMe to undergo transitions between right-handed to left-handed helical conformers were explored with higher-temperature simulations. This was an expedient approach to observing the infrequent conformational transitions between helical states; while the free energy landscape will differ somewhat at the higher temperature, these preliminary studies facilitate future detailed studies of the transitions using umbrella sampling and/or replica exchange. All observed pathways went through a higher-energy state where the φ angle approaches 180°. The 500 K simulations provide potential reaction pathways for Aib to undergo transitions between the left-handed and right-handed helix. Multiple pathways were accessible in the simulation, and the most likely and lowest-energy pathways are shown in Figure 10.

Acknowledgment. We are indebted to Dr. Robert Woody, who provided us with some important suggestions concerning the interpretation of the ECD spectra at an early stage of the project. The Ac-Aib-OMe potential energy plot was generously provided by Daniel J. Kuster of the Marshall Lab. This research was supported in part by an NIH research grant (GM 08460) to G.R.M. J.F. also acknowledges graduate support from the

(83) Benedetti, E.; Bavoso, A.; DiBasio, B.; Pavone, V.; Pedone, C.; Crisma, M.; Bonora, G. M.; Toniolo, C. *J. Am. Chem. Soc.* **1982**, *104*, 2437.
(84) Pispisa, B.; Palleschi, A.; Amato, M. E.; Segre, A. L.; Vernanzi, M. *Macromolecules* **1997**, *30*, 4905.

Division of Biology and Biomedical Science of Washington University in St. Louis, the Computational Biology Training Grant (GM 008802), and the Kauffman Foundation. Computation resources were provided in part by grants from Teragrid. The research in the laboratory of R.S.S. was partially supported by a grant from the National Science Foundation (MCB 0318749).

Supporting Information Available: The description of peptide synthesis and three figures exhibiting the results of MD simulations. This material is available free of charge via the Internet at http://pubs.acs.org.

JA0738430